Impact of process and physico-chemical conditions on the formation of curcumin-whey protein composite particles capable to stabilize food-compatible oil in water emulsions

Aditya Nayak, Claude Genot, Anne Meynier, Angélina Dorlando, Isabelle Capron

Impact of process and physico-chemical conditions on the formation of curcumin-whey protein composite particles capable to stabilize food-compatible oil in water emulsions

Aditya Nayak*, Claude Genot, Anne Meynier, Angélina Dorlando, Isabelle Capron

INRAE, UR BIA, F-44316, Nantes, France

Corresponding Author: Isabelle Capron, UR1268 Biopolymères Interactions Assemblages, INRAE, F-44316 Nantes, France.
E-mail: Isabelle.capron@inrae.fr.
Phone: +33 (0) 2 40 67 50 95
Fax : +33 (0) 2 40 67 50 43

Aditya Nayak : UR1268 Biopolymères Interactions Assemblages, INRA, F-44316 Nantes, France.
E-mail: adityatorke@gmail.com
Phone : +91 9148043556

Abbreviations

WPI: Whey protein isolate

NWp: Native whey protein

DWp: Denatured whey protein

CNp: Curcumin native whey protein

CDp: Curcumin denatured whey protein

CWP: Curcumin-whey protein

o/w: oil-in-water

⁎Current Affiliation: Corporate R&D, ITC Life Science and Technology Centre, Bangalore-560058, India

Abstract

Use of nanonized curcumin-whey protein (CWP) composite particles as Pickering stabilizers are an attractive strategy due to their edibility and natural origin. This study aimed to examine the effect of physico-chemical conditions (pH, ionic strength, protein form) during the formation of CWP composite nanoparticles on their physico-chemical characteristics (size, surface charge, morphology) and further their Pickering ability by influencing their aptitude to stabilize oil/water interfaces.

Our study demonstrated that, to favor the protein-curcumin interactions and to improve the particle characteristics (smaller size, monodispersity), one should increase the accessibility of hydrophobic moiety of proteins (denaturation) and control ionic strength. Increasing the concentration of the CWP composite nanoparticles decreased size and polydispersity enhancing emulsion stability. Use of these CWP composite nanoparticles in food products with high ionic strength will tend to flocculation and thereby emulsions destabilization.

This work allows for a better understanding of the role of physico-chemical conditions on the formation of CWP composite nanoparticles and thereof their oil/water interfacial activity.

Key words: Curcumin, oil-in-water emulsion, Pickering stabilization, whey protein, composite nanoparticles

1. Introduction

In the last decade, colloidal particles have been extensively used to stabilize biphasic dispersions like emulsions and foams owing to their ability to accumulate at the liquid/liquid or air/liquid interface (Binks et al., 2006; Capron I., Rojas O. J., and Bordes R., 2017; Lam S., Velikov K. P., and Velev O. D., 2014). In these systems known as Pickering emulsions, colloidal particles absorb at the interface forming a physical barrier (Schröder A., Sprakel J., Schroën K., Spaen J. N., and Berton-Carabin C. C., 2018).

Up today, various edible and non-edible components, for example, clay, silica particles, cellulose, chitosan, polyphenols, fat crystals, etc., have been used as colloidal particles to stabilize water-in-oil, oil-in-water or double emulsions and foams (Berton-Carabin C. C. and Schroën K., 2015; McClements D. J. and Decker E. A., 2000). Among the edible colloidal particles, polyphenols are gaining higher interest due to their recognized acceptability by consumers due to their natural origin (label friendly) (Aditya et al., 2017; Duffus et al., 2016; Zembyla et al., 2018). Further, they are easily available and cost effective (Aditya N. P., Hamilton I. E., and Norton I. T., 2017). In this regard, the use of curcumin, a polyphenol known for its health benefits as a Pickering particle is an attractive strategy because it will not only physically stabilize the emulsions, but its consumption is also associated with several health benefits like anti-inflammatory, anti-diabetic, anti-parasitic, etc., (Aditya et al., 2015; Nayak et al., 2016). Curcumin tends to form large and highly polydispersed particles that present insolubility in water and most organic solvents and limited wettability in both the continuous and dispersed fluid phases. This compromises their interfacial packing ability. As a consequence, a high concentration of curcumin is required to

stabilize biphasic dispersions and it results in droplets of several microns, which compromises their applicability in the processed food products (Aditya et al., 2017; Luo Z. *et al.*, 2011) .

These last years, it has been demonstrated that, curcumin particles of controlled shape and size can be prepared by nanonization technology in order to modulate their Pickering ability. This nanonization was achieved by mixing curcumin with edible materials like whey protein isolate (WPI) and green chemicals like water and ethanol. These engineered curcumin particles were successfully used to form oil-in-water droplets with diameter ~2 µm (Aditya et al., 2017).

Nanonization can be accomplished either by a top-down approach (high pressure homogenization, microfluidization, media milling, etc.) or bottom-up approach (precipitation with a non-solvent or supercritical fluids and precipitation by solvent removal) (Aditya, Yang, Kim, & Ko, 2015; Sinha, Müller, & Möschwitzer, 2013). The bottom-up approach which is generally known as a precipitation allows building particles from the molecular level; thus it doesn't only enable the reduction of the particle size but also allows obtaining particles differing in shape, surface morphology, etc. In this regard, Kakran et al., 2010 developed an approach to fabricate nanosuspension by evaporative precipitation using rotary vacuum evaporator (Kakran, *et al.,* 2010). Usually, in this technique, solvent and non-solvent are admixed and the solvent evaporated rapidly to obtain a colloidal suspension.

Both curcumin and proteins (WPI) used in this study are sensitive to physico-chemical conditions such as pH, ionic strength, protein form (native or denatured), etc (Aditya, Yang, Kim, & Ko, 2015; Hussain, Gaiani, Jeandel, Ghanbaja, & Scher, 2012; Nayak et al., 2016). Thus, we hypothesized that, prevailing physico-chemical conditions like pH (pH 3 - 10), protein form (native or denatured) and ionic strength (40 - 100 mM)) will play an important role in determining the particle characteristics (size, surface charge, morphology, etc) by driving the

interaction between the protein (WPI) and the polyphenol (curcumin) and thereof their ability to form oil-in-water Pickering emulsion and emulsion characteristics. In this study, thus, physico-chemical conditions on particle characteristics during nanonization in terms of size, surface charge, interaction between curcumin and stabilizer and short term stability was explored. In the second stage, emulsions were fabricated using these engineered curcumin particles and were characterized for their droplet size, size distribution and morphology.

2. Materials and Methods

2.1. Materials. Low heat whey protein powder was obtained from LACTALIS Ingredients (France) as gift sample, designed as WPI. It contained 88.5 wt% of proteins made up of 12wt% of caseins and 88% of whey proteins. Other components are 5.1% moisture, ≤ 3% lactose, < 3% minerals and ≤ 0.4% fat. pH of the protein solution was adjusted with either NaOH or HCl. Commercially available rapeseed oil was purchased from a local supermarket. Curcumin, sodium chloride and calcium chloride were of analytical grade and purchased from Sigma-Aldrich. Anhydrous ethanol (purity 99.9 vol%) was obtained from Sigma-Aldrich. All chemicals were used as received. Deionized water (< 0.2 μS/cm) was used from a 115 Millipore Synergy purification system.

2.2. Preparation of curcumin-whey protein (CWP) composite nanoparticles

Non-solvent precipitation technique was used to fabricate CWP composite nanoparticles as described earlier (Kakran M. *et al.*, 2010). Curcumin was dissolved in ethanol (3 mg/mL), which acted as a solvent phase. This solvent phase was added to the water in which 0.3 g/L WPI was dissolved. This acted as a non-solvent phase. Immediately, solvent (ethanol) was evaporated from

the mixture of solvent and non-solvent with Rota evaporator under vacuum condition. This resulted in the supersaturation and particles were suspended in the non-solvent (supplementary Figure S1). These experiments were carried out with 500mL round bottom flask and maximum solution (solvent + non-solvent) was 50 mL. The effect of solvent evaporation rate on particle characteristics (mean size and size distribution) was initially studied by applying various levels of vacuum pressure (35 to 120 mbar). Solvent evaporation was confirmed by measuring the total volume of non-solvent remaining in the round bottom flask. Total time taken to evaporate the solvent was 120 s at 35 mbar, 150 s at 50 mbar, 180 s at 70 mbar and 240s at 120 mbar.

To evaluate the effect of protein form, whey protein solution was denatured by heating it for 30 minutes at 85 ^{0}C in a water bath. The denatured protein solution was then cooled to room temperature. Further, physico-chemical conditions *e.g*., curcumin concentration (0.15, 0.30 and 0.60 g/L), cation type (monovalent Na^{+} and divalent Ca^{++}) and concentration, and pH (3, 7 and 10) on the physico-chemical characteristics of the CWP composite nanoparticle was studied (Table 1).

All samples were stored in the dark at 4 °C until further analysis. The particles were stable for at least one month (supplementary Figure S1). Detailed characteristics of all formulations are summarized in table 1.

2.3. Preparation of CWP stabilized emulsions

The oil-in-water (o/w) emulsions were prepared with rapeseed oil and CWP composite nanoparticle aqueous suspension as described earlier with the required modification (Cherhal F., Cousin F., and Capron I., 2016). For all experiments, 40 g emulsions were prepared at oil/aqueous phase ratios of 20/80 (w/w). Briefly, 32 g of curcumin-WPI composite aqueous

suspension was poured in a glass beaker and 8 g of rapeseed oil was added slowly under high-speed homogenization. Homogenization was carried out at 20000 rpm for 6 minutes (Heidolph Silent Crusher M homogenizer, Germany). Immediately after, the coarse emulsion was subjected to sonication. Sonication was carried out for 6 s (2s on/2s off) at amplitude 6 with 3 mm titanium probe. Control emulsions were fabricated with only native or denatured protein without curcumin (Table 1). Emulsions were stored at 4 °C in darkness until further analysis.

2.4. CWP nanoparticle size and ζ-potential analysis

CWP composite nanoparticles size and size distribution were measured by dynamic light scattering (DLS) using a Malvern Zetasizer NanoZS (Malvern Instruments, U.K.). Samples were diluted (1:100 v/v) with ultrapure water just before analysis to yield a suitable scattering intensity and put in 1 mL polystyrene semi-micro cuvettes with 10 mm optical pathway (Ratiolab® cuvets, semi-micro PS no. 2712120). The scattering intensity was measured at 25°C in backscattering mode with an angle of 173° relative to the source. The refractive index and absorption coefficient of the curcumin were fixed respectively at 1.42 and 0.01. The parameters of pure water at 25°C were used for the dispersing medium (viscosity=0.8872cP; refractive index=1.330). The volume mean size (vol %) obtained from the zetasizer was used for data interpretation.

The ζ-potential of CWP composite nanoparticles was measured with a Malvern Zetasizer NanoZS (Malvern Instruments, U.K.) without dilution before the measurement.

2.5. Emulsion characterization

Volume averaged droplet diameter ($D_{4,3}$), surface averaged droplet diameter ($D_{3,2}$) and droplet size distribution of the o/w Pickering emulsions were measured by laser light diffraction with a

Horiba Scientific LA-960 Pratica granulometer equipped with a He–Ne laser and calculated with refractive index 1.47 for rapeseed oil. The emulsions were diluted in water to obtain optimal scattering intensity. All measurements were performed at 25 ^{0}C.

2.6. Transmission Electron Microscopy (TEM) and Wet Scanning Transmission Electron Microscope (Wet-STEM).

A total of 10 µL of CWP composite nanoparticles suspennded was deposited on freshly glow-discharged carbon-coated electron microscope grids (200 mesh, Delta Microscopies, France) for 2 min, the excess water were removed with filter paper. The sample was then immediately negatively stained with phosphotungstic solution (2% w/v) for 2 min and dried after absorbing excessive phosphotungstic solution with filter paper. The grids were observed with a Jeol JEM 1230 TEM at 80 kV. The software ImageJ® was used for image analysis. The raw TEM images were binarised by thresholding techniques to classify, which pixels belonged to particle regions, the perimeter of each particle was then delimited and finally the particles counted by an automatic process.

2.7. Front-Face Fluorescence Measurements.

Spectrophotometer (F-4500 FL Spectrophotometer, Hitachi) equipped with a front-surface accessory was used to record fluorescence emission spectra of native and denatured WPI and CWP composite nanoparticles suspended without any further dilution. The spectra were recorded from 395 to 600 nm with a 1 nm step, with the excitation wavelength set at 290 nm with 2.5 nm emission and excitation slits. All spectra were automatically corrected from instrumental

distortions in emission and excitation and smoothed when required (Peakfit software, 4th version, Jandel Scientific, Chicago, IL). Spectra were measured at 20 ± 1 °C.

2.8. Statistical analysis

Experiments were carried out in duplicate or triplicate. The mean and standard deviation (SD) of the mean were calculated from replicates. The statistical difference between the two groups was evaluated using the Student's t-test. A probability value of <0.05 was considered significant. All the statistical analyses were performed using Microsoft Excel for Mac 2011.

3. Results and Discussion

3.1. Production and characterization of CWP composite nanoparticle

Usually, in nanoprecipitation technology, solvents and non-solvents are admixed and solvent evaporated rapidly to obtain a colloidal suspension(Kakran M., Sahoo N. G., Li L., Judeh Z., Wang Y., Chong K., and Loh L., 2010). However, processing parameters such as solvent evaporation rate play a crucial role in determining the quality of the formed nanoparticles since they influence the supersaturation, nucleation and particle formation phenomenon.

Thus, we studied first the effect of solvent evaporation rate on the particle formation. Different solvent evaporation rates from the mixture of solvent (ethanol) and non-solvent (water) were obtained by varying the vacuum level from 35 to 120 mbar. As shown in Figure 1A, as the vacuum level decreased from 120 to 35 mbar, the mean particle size of the protein-curcumin nanoparticles decreased significantly ($p < 0.05$) from 436 ± 44 nm to 177 ± 26 nm. This can be attributed to the faster solvent evaporation at greater vacuum pressure. It resulted, for all vacuum

conditions, in the shift of the global size into monodispersed nanoparticles of varying average diameter, as evidenced from the narrow size distribution (Figure 1B). This is in agreement with the LaMer-mechanism (LaMer V. K. and Dinegar R. H., 1950). According to LaMer-mechanism, preparation of a colloidal dispersion, by condensation of initially formed monomer, involves three steps i.e., supersaturation, nucleation and particle growth. By obtaining a high degree of supersaturation by rapid solvent evaporation, a brief outburst of nucleation can be achieved. This results in the formation of a higher number of smaller nuclei, which further uniformly grow into particles by diffusional growth. Thus, faster solvent evaporation by increasing the vacuum pressure resulted in the formation of smaller particles.

Further, the effect of solvent to non-solvent ratio on the characteristics of the curcumin colloidal dispersion was studied (Figure 2). At the ratio of 1:20 and native WPI, The mean particle size was ~140 nm, whereas, at 1:5 ratios, it was ~260 nm. Similarly, when a denatured protein was used, upon reducing the ratio of solvent in the mixture of solvent and anti-solvent from 1:5 to 1:20 (v/v), particles of smaller mean size with narrow size distribution were formed. Thus, in accordance with the earlier studies, when the solvent ratio (ethanol solution of curcumin at 3g/L) to non-solvent (aqueous solution of WPI at 0.3 g/L) ratio was decreased from 1:5 to 1:20 (v/v), particles became significantly ($p < 0.05$) smaller and monodispersed (narrow size distribution)(Aditya N. P., Hamilton I. E., Noon J., and Norton I. T., 2019). This could be due to the formation of a higher number of nuclei when the solvent to non-solvent ratio is increased. This reduces the diffusion distance between two nuclei resulting in increased particle collisions leading to particle aggregation (Aditya N. P., Yang H., Kim S., and Ko S., 2015; Wang Y., Song J., Chow S. F., Chow A. H. L., and Zheng Y., 2015). Another potential reason may be that a lesser amount of protein is available to stabilize the particles at 1:5 (v/v) solvent to non-solvent

ratio in comparison to 1:20 (v/v) ratio. For example, at 1:5 solvent to non-solvent ratio, 1 molecule of protein has to stabilize ~108 curcumin molecules. At 1:20 solvent to non-solvent ratio, 1 protein molecule has to stabilize only ~27 curcumin molecules. This leads probably to insufficient interfacial covering at 1:5 ratio, which in turn leads to particle aggregation and increases the mean particle size.

Particle size is one among the most important parameters, which determines the efficiency of the particle adsorption at the oil–water interface. It was established that, the larger the particles, the higher the adsorption energy and the stronger the anchoring at the interface. Whereas, smaller particle limit coalescence due to their higher packing efficiency at the interface (Aditya N. P., Hamilton I. E., and Norton I. T., 2017; Duffus L. J., Norton J. E., Smith P., Norton I. T., and Spyropoulos F., 2016).

As shown in Figure 3A, when denatured protein was used as a stabilizer, mean particle sizes of the formed particles were slightly but significantly ($p<0.05$) smaller (155 ± 3 nm) in comparison to native protein (185 ± 4 nm). This may be because hydrophobic moieties of the protein is exposed when whey protein is denatured. This would increase the interaction between hydrophobic moieties of the protein and the hydrophobic curcumin which is investigated and discussed in detail later in the manuscript (Sneharani A. H., Karakkat J. V., Singh S. A., and Rao A. G. A., 2010). Earlier studies have shown that protein-polyphenol interactions are mainly due to hydrophobic bonding between aromatic and phenolic rings of polyphenols and hydrophobic amino acid residues of proteins like tryptophan (Siebert K. J., Troukhanova N. V., and Lynn P. Y., 1996).

Presence of ionic strength has also a profound effect on the particle size (size and size distribution) and stability. As shown in Figure 3A, when NaCl is used at 40, 80 or 100 mM

(pH=7), formed particles are significant ($p<0.05$) smaller with a diameter of 140 nm. This is attributed to the ion induced protein condensation resulting in the size reduction(Hussain R., Gaiani C., Jeandel C., Ghanbaja J., and Scher J., 2012; Smirnov I. V., Dimitrov S. I., and Makarov V. L., 1988). Multivalent salts are expected to induce higher aggregation compared to monovalent salt. Thus, $CaCl_2$ was used at 40 mM. Dynamic light scattering measurements of the formed particles gave a mean size above 1 µm with polydispersity index of >1, characteristic of the size distribution of aggregates and not of individual particles, the values being not represented in Figure 3A. Ca^{++} divalent ion was thus expectedly much more efficient in inducing aggregation than the monovalent ones. This is due to the charge screening effect, which neutralizes the surface charge, and also allows ionic bridging between proteins. Thus, it promotes protein aggregation (Bhat R. and Ahluwalia J. C., 1987; Ju Z. Y. and Kilara A., 1998).

Surface charge is one of the potential factors which not only affect the stability of the particles, but also their behavior at the oil-water interface (Duffus L. J., Norton J. E., Smith P., Norton I. T., and Spyropoulos F., 2016). Thus, ζ-potential of the CWP nanoparticles dispersed in water was studied.

As shown in Figure 3B, when either native or denatured proteins were used as stabilizers without monovalent salt, CWP nanoparticles were anionic (~ -40 mV) in both neutral and alkaline conditions. However, the isoelectric point of major whey proteins being in the range 4.5-5.2, they showed positive surface charge (~ +45 mV) at pH 3. When NaCl was added to the colloid dispersion at neutral pH, surface charge was significantly ($p <0.05$) reduced compared to the formulation without NaCl at the same pH. This reduction in surface charge is due to the binding of ions to the charged protein moiety, which causes electrostatic screening (Binks B. P., Murakami R., Armes S. P., and Fujii S., 2006; Tangsuphoom N. and Coupland J. N., 2008).

Regarding the effect of divalent salt on the particle surface charge, it was not possible to check the surface charge of the CWP particles, because the aggregated colloidal dispersion flocculated as clumps.

TEM and Wet-STEM were used to visually observe the morphology of the CWP nanoparticles. In accordance with the dynamic light scattering data, TEM and wet-STEM observation confirmed the formation of monodispersed (in comparison to unprocessed curcumin particles in native form) and nano-range particles, which were spherical in shape (Figure 4 and Supplementary figure S2). This also endorsed that the, after nanonization size of curcumin particles was reduced significantly ($p < 0.05$) (unprocessed curcumin particles in native form were of ~ 15µm size). In this regard, formed curcumin particles have favorable particle characteristics (small size, spherical shape and monodispersed) in comparison to their unprocessed curcumin particles to enhance the interfacial activity.

An interaction of the WPI with curcumin was investigated using front-face fluorescence spectroscopy by studying intrinsic fluorescence properties of tryptophanyl residues (Trp) of the proteins. Change in the emission spectra of Trp is generally studied to evaluate the change in the structure of proteins; for example, changes of fluorescence intensity, blue shift, or red shift provide useful information about the effect of Trp microenvironment and thus about the proteins structure and their interaction with other molecules (Rahimi Yazdi S. and Corredig M., 2012). Because curcumin nanoparticles gave the systems very high turbidities, high dilution levels of samples would have been needed to reach absorbencies less than 0.1 (or better 0.05), as required to minimize inner-filter effects due to absorption of excitation and emission lights in classical right-angle mode. At these high dilution factors, protein concentration would have been too low regarding the sensitivity of the apparatus to detect protein fluorescence. Thus, an original method

was used where fluorescence measurements were performed in a front-face mode without any dilution of samples. In that mode, only a thin layer of the sample is irradiated and emission spectra, including emission intensities can be compared directly, provided similar organization and total absorbance(Garimella Purna S. K., Prow L. A., and Metzger L. E., 2005) (Genot et al 1992).

To start with, the effect of physico-chemical conditions on emission fluorescence spectra (excitation wavelength set at 295 nm) of the protein without curcumin. As shown in Figure 5A, WPI, in its native form at neutral pH (pH7) exhibited a maximum wavelength (λmax) at 328 nm. Thermal denaturation of WPI resulted in the increased Trp fluorescence and λmax was shifted to 335 nm. This red-shift of λmax is attributed to a greater exposure of Trp to the aqueous polar environment, while in the native proteins the residues are mostly buried inside in a mostly nonpolar environment as indicated by the λmax below 330 nm. Similarly, at acidic pH (pH 3), we observed a shift to 333 nm. When monovalent salt (Na^+) was added to native WPI solution, a decrease in fluorescence intensity was observed and λmax was moderately shifted to 327 nm. This blue shift confirms that, in the presence of monovalent salt, Trp is confined within a non-polar environment. In agreement with our earlier assumption that, decrease in curcumin particle size is due to protein condensation. Protein condensation favors internal interactions between amino acids and leads to quenching of Trp fluorescence due to increased vicinity with neighbors (see figure 3A).

Later, the effect of these different physico-chemical conditions on the interactions of curcumin with WPI was studied. As shown in Figure 5B, the presence of curcumin significantly ($p < 0.05$) quenched the Trp fluorescence (maximum fluorescence intensity > 3000 A.U. decreasing to less than 200 A.U.) which evidences the binding of curcumin to WPI proteins. This is in agreement

with the earlier studies that also showed a decrease in Trp fluorescence due to interaction between protein and hydrophobic molecules(Chen W. *et al.*, 2019; Rahimi Yazdi S. and Corredig M., 2012). This decrease is more prominent when WPI was denatured. This observation is in agreement with earlier observations that denaturation exposes hydrophobic moieties of proteins to the aqueous environment, which favors the interaction between these hydrophobic moieties of the proteins and the hydrophobic curcumin.

At pH 3.0, in comparison to other formulations, quenching of Trp fluorescence was minimal in the presence of curcumin. This may be attributed to the different solubility of proteins and curcumin and also surface charge. In acidic pH, proteins are more hydrophilic (above or below their isoelectric point, proteins prefer to interact with water); whereas curcumin is hydrophobic, which decreases the interactions between proteins and curcumin. Additionally, at acidic pH, both curcumin and WPI are cationic(Mohammadian M. *et al.*, 2019; Zembyla M., Murray B. S., and Sarkar A., 2018). This decreases the binding capacity of curcumin with WPI resulting in the minimal quenching of the Trp fluorescence.

To support our explanation that decrease in Trp fluorescence is due to the interactions between WPI and curcumin, we studied the effect of curcumin concentration on the protein Trp fluorescence. As shown in Figure 6A, quenching of the Trp fluorescence of native WPI depends on curcumin concentration. Quenching of the Trp fluorescence was minimum at the curcumin concentration of 0.15 g/L and it was maximum at 0.60 g/L. A red shift of ~7 nm of the maximum emission wavelength was also observed. In addition, as shown in the Figure 6B, the greater decrease in Trp fluorescence with denaturated WPI in comparison to native WPI indicates that interactions of curcumin and WPI were increased. This may be attributed to the increase in accessibility of hydrophobic moieties due to the unfolding of the WPI, which facilitated the

interactions between WPI and curcumin. This is in agreement with earlier results that show that curcumin binds to the nonpolar regions of proteins (Rahimi & Corredig., 2012).

3.2. Production and characterization of CWP composite nanoparticle stabilized oil-in-water emulsion

Oil-in-water emulsions were produced with the CWP composite nanoparticles as stabilizer. All the emulsions were formed at the oil to water wt% ratio of 20:80 (supplementary Figure S3). Control emulsions stabilized by native or denaturated WPI only (0.3 g/L) were also prepared (NWp and DWp in Figure 7A). As shown in Figure 7, when emulsions were prepared with 354 only 0.3 g/L of WPI, the mean droplet diameter was in the range of 20 to 25 µm (Figure 7A) with a very large and polydisperse distribution of droplet diameters (Figure 7B). When emulsions were prepared with CWP composite particles used as a stabilizer at 0.15, 0.30 and 0.60 g/L, the average droplet diameters were ~15, 10 and 5 µm respectively. Increase in amounts of CWP composite nanoparticles resulted in the formation of droplets with narrower size distributions in a concentration-dependent manner (Fig 7B). This significant ($p<0.05$) decrease in size of the droplets upon increasing the particle concentration and narrowing of the size distribution is attributed to the so-called limited coalescence effect. The availability of a sufficient number of particles in the continuous phase are required to swiftly cover and stabilize newly formed droplets and thereby avoid in-processing coalescence(Arditty S., Whitby C. P., Binks B. P., Schmitt V., and Leal-Calderon F., 2003). However, no significant difference was observed when droplets were formed using either native or denatured protein stabilized CWP composite nanoparticles. Similarly, the effect of pH on the droplet formation was also non-significant.

When CWP nanoparticles prepared in the presence of NaCl were used as a stabilizer, droplet diameter and droplet diameter distribution significantly increased with increasing NaCl concentration (Figures 7A and 7C). At 40 mM NaCl concentration, mean diameters of obtained droplets were ~10 µm, whereas it increased to ~18 µm when 100 mM NaCl was used. The observed increase in size indicated that droplets aggregation and/or coalescence due to charge screening effect of salt which is evidenced from the ζ-potential measurement of CWP nanoparticles. This aggregation is attributed to the charge neutralization by the sodium chloride leading to droplet-droplet binding through low energy interactions and flocculation (Binks B. P., Murakami R., Armes S. P., and Fujii S., 2006; Ju Z. Y. and Kilara A., 1998; Tangsuphoom N. and Coupland J. N., 2008). This is per the observation that the addition of NaCl resulted in a reduction of the CWP nanoparticles' surface charge (Figure 3B). When CWP composite nanoparticles were prepared with $CaCl_2$, unstable droplets of~70 µm formed clumps soon after preparation which was visible to the naked eye.

4. Conclusion

Previous work showed that nanonization technology can be used to enhance the Pickering ability of the curcumin particles and successfully used engineered particles to stabilize water continuous emulsions (N. P. Aditya et al., 2017).

In the present study, It was identified the effect of i) several formulation parameters, i.e. curcumin concentration, pH and ionic strength, presence of monovalent or divalent ions, native or denatured proteins, and ii) process parameters, i.e. solvent evaporation rate, solvent to non solvent ratio. The characteristics (size distribution, aggregation) of the CWP composite nanoparticles are correlated to those of Pickering emulsions formed

using these colloid particles.

This study clearly shows that to favor the protein-curcumin interactions and improve the particle characteristics (smaller size, monodispersity), one should increase the accessibility of hydrophobic moiety of proteins (denaturation) to curcumin and to use enough ionic strength. Further, increasing the concentration of the CWP composite nanoparticles improves droplet characteristics (size and monodispersity) and use of this CWP composite nanoparticles in high ionic strength conditions may weaken the system due to emulsions destabilization by charge screening effect of ions.

This new knowledge of edible particle preparation and their Pickering ability in accordance with the physicochemical conditions like ionic strength, pH etc., of the specific food products will have far-reaching implications on the rational selection of Pickering stabilized emulsions for application. Further, we believe that this research outcome will have further important inferences on the Pickering particles selection criteria for the stabilization of simple and double emulsions.

Acknowledgement

"Aditya has received the support of the EU in the framework of the Marie-Curie FP7 COFUND People Programme, through the award of an AgreenSkills+ fellowship under grant agreement no "609398". Authors also thank Region Pays-de-la-Loire for support (RFI Food-For-Tomorrow). Lucie Ribourg, Michèle Viau, Alice Kermarrec and Nadege Beury from Biopolymères Interactions Assemblages, INRA are thanked for their help with instrumental training and scientific discussion.

References

Aditya N. P., Aditya S., Yang H.-J., Kim H. W., Park S. O., Lee J., & Ko S. (2015). Curcumin and catechin co-loaded water-in-oil-in-water emulsion and its beverage application. *Journal of Functional Foods, 15*, 35-43. doi:https://doi.org/10.1016/j.jff.2015.03.013

Aditya N. P., Hamilton I. E., Noon J., & Norton I. T. (2019). Microwave-Assisted Nanonization of Poorly Water-Soluble Curcumin. *ACS Sustainable Chemistry & Engineering, 7*(11), 9771-9781. doi:10.1021/acssuschemeng.8b06377

Aditya N. P., Hamilton I. E., & Norton I. T. (2017). Amorphous nano-curcumin stabilized oil in water emulsion: Physico chemical characterization. *Food Chemistry, 224*, 191-200. doi:https://doi.org/10.1016/j.foodchem.2016.12.082

Aditya N. P., Yang H., Kim S., & Ko S. (2015). Fabrication of amorphous curcumin nanosuspensions using β-lactoglobulin to enhance solubility, stability, and bioavailability. *Colloids and Surfaces B: Biointerfaces, 127*, 114-121. doi:https://doi.org/10.1016/j.colsurfb.2015.01.027

Arditty S., Whitby C. P., Binks B. P., Schmitt V., & Leal-Calderon F. (2003). Some general features of limited coalescence in solid-stabilized emulsions. *Eur. Phys. J. E, 12*(2), 355. Retrieved from https://doi.org/10.1140/epje/i2003-10060-4

Berton-Carabin C. C., & Schroën K. (2015). Pickering Emulsions for Food Applications: Background, Trends, and Challenges. *Annual Review of Food Science and Technology, 6*(1), 263-297. doi:10.1146/annurev-food-081114-110822

Bhat R., & Ahluwalia J. C. (1987). Effect of calcium chloride on the conformation of proteins. Thermodynamic studies of some model compounds. *Int J Pept Protein Res, 30*(2), 145-152. Retrieved from http://www.ncbi.nlm.nih.gov/pubmed/3679668

Binks B. P., Murakami R., Armes S. P., & Fujii S. (2006). Effects of pH and Salt Concentration on Oil-in-Water Emulsions Stabilized Solely by Nanocomposite Microgel Particles. *Langmuir, 22*(5), 2050-2057. doi:10.1021/la053017+

Capron I., Rojas O. J., & Bordes R. (2017). Behavior of nanocelluloses at interfaces. *Current Opinion in Colloid & Interface Science, 29*, 83-95. doi:https://doi.org/10.1016/j.cocis.2017.04.001

Chen W., Wang W., Ma X., Lv R., Balaso Watharkar R., Ding T., . . . Liu D. (2019). Effect of pH-shifting treatment on structural and functional properties of whey protein isolate and its interaction with (−)-epigallocatechin-3-gallate. *Food Chemistry, 274*, 234-241. doi:https://doi.org/10.1016/j.foodchem.2018.08.106

Cherhal F., Cousin F., & Capron I. (2016). Structural Description of the Interface of Pickering Emulsions Stabilized by Cellulose Nanocrystals. *Biomacromolecules, 17*(2), 496-502. doi:10.1021/acs.biomac.5b01413

Duffus L. J., Norton J. E., Smith P., Norton I. T., & Spyropoulos F. (2016). A comparative study on the capacity of a range of food-grade particles to form stable O/W and W/O Pickering emulsions. *Journal of Colloid and Interface Science, 473*, 9-21. doi:https://doi.org/10.1016/j.jcis.2016.03.060

Garimella Purna S. K., Prow L. A., & Metzger L. E. (2005). Utilization of Front-Face Fluorescence Spectroscopy for Analysis of Process Cheese Functionality. *Journal of Dairy Science, 88*(2), 470-477. doi:https://doi.org/10.3168/jds.S0022-0302(05)72708-9

Hussain R., Gaiani C., Jeandel C., Ghanbaja J., & Scher J. (2012). Combined effect of heat treatment and ionic strength on the functionality of whey proteins. *Journal of Dairy Science, 95*(11), 6260-6273. doi:https://doi.org/10.3168/jds.2012-5416

Ju Z. Y., & Kilara A. (1998). Aggregation Induced by Calcium Chloride and Subsequent Thermal Gelation of Whey Protein Isolate. *Journal of Dairy Science, 81*(4), 925-931. doi:https://doi.org/10.3168/jds.S0022-0302(98)75652-8

Kakran M., Sahoo N. G., Li L., Judeh Z., Wang Y., Chong K., & Loh L. (2010). Fabrication of drug nanoparticles by evaporative precipitation of nanosuspension. *Int J Pharm, 383*(1-2), 285-292. doi:10.1016/j.ijpharm.2009.09.030

Lam S., Velikov K. P., & Velev O. D. (2014). Pickering stabilization of foams and emulsions with particles of biological origin. *Current Opinion in Colloid & Interface Science, 19*(5), 490-500. doi:https://doi.org/10.1016/j.cocis.2014.07.003

LaMer V. K., & Dinegar R. H. (1950). Theory, Production and Mechanism of Formation of Monodispersed Hydrosols. *Journal of the American Chemical Society, 72*(11), 4847-4854. doi:10.1021/ja01167a001

Luo Z., Murray B. S., Yusoff A., Morgan M. R. A., Povey M. J. W., & Day A. J. (2011). Particle-Stabilizing Effects of Flavonoids at the Oil−Water Interface. *Journal of Agricultural and Food Chemistry, 59*(6), 2636-2645. doi:10.1021/jf1041855

McClements D. J., & Decker E. A. (2000). Lipid Oxidation in Oil-in-Water Emulsions: Impact of Molecular Environment on Chemical Reactions in Heterogeneous Food Systems. *Journal of Food Science, 65*(8), 1270-1282. doi:doi:10.1111/j.1365-2621.2000.tb10596.x

Mohammadian M., Salami M., Momen S., Alavi F., Emam-Djomeh Z., & Moosavi-Movahedi A. A. (2019). Enhancing the aqueous solubility of curcumin at acidic condition through the complexation with whey protein nanofibrils. *Food Hydrocolloids, 87*, 902-914. doi:https://doi.org/10.1016/j.foodhyd.2018.09.001

Nayak A. P., Mills T., & Norton I. (2016). Lipid Based Nanosystems for Curcumin: Past, Present and Future. *Curr Pharm Des, 22*(27), 4247-4256. Retrieved from http://www.ncbi.nlm.nih.gov/pubmed/27306091

Rahimi Yazdi S., & Corredig M. (2012). Heating of milk alters the binding of curcumin to casein micelles. A fluorescence spectroscopy study. *Food Chemistry, 132*(3), 1143-1149. doi:https://doi.org/10.1016/j.foodchem.2011.11.019

Schröder A., Sprakel J., Schroën K., Spaen J. N., & Berton-Carabin C. C. (2018). Coalescence stability of Pickering emulsions produced with lipid particles: A microfluidic study. *Journal of Food Engineering, 234*, 63-72. doi:https://doi.org/10.1016/j.jfoodeng.2018.04.007

Siebert K. J., Troukhanova N. V., & Lynn P. Y. (1996). Nature of Polyphenol−Protein Interactions. *Journal of Agricultural and Food Chemistry, 44*(1), 80-85. doi:10.1021/jf9502459

Smirnov I. V., Dimitrov S. I., & Makarov V. L. (1988). NaCl-Induced Chromatin Condensation. Application of Static Light Scattering at 90° and Stopped Flow Technique. *Journal of Biomolecular Structure and Dynamics, 5*(5), 1127-1134. doi:10.1080/07391102.1988.10506453

Sneharani A. H., Karakkat J. V., Singh S. A., & Rao A. G. A. (2010). Interaction of Curcumin with β-Lactoglobulin—Stability, Spectroscopic Analysis, and Molecular Modeling of the

Complex. *Journal of Agricultural and Food Chemistry, 58*(20), 11130-11139. doi:10.1021/jf102826q

Tangsuphoom N., & Coupland J. N. (2008). Effect of pH and ionic strength on the physicochemical properties of coconut milk emulsions. *J Food Sci, 73*(6), E274-280. Retrieved from http://www.ncbi.nlm.nih.gov/pubmed/19241548

Wang Y., Song J., Chow S. F., Chow A. H. L., & Zheng Y. (2015). Particle size tailoring of ursolic acid nanosuspensions for improved anticancer activity by controlled antisolvent precipitation. *International Journal of Pharmaceutics, 494*(1), 479-489. doi:https://doi.org/10.1016/j.ijpharm.2015.08.052

Zembyla M., Murray B. S., & Sarkar A. (2018). Water-In-Oil Pickering Emulsions Stabilized by Water-Insoluble Polyphenol Crystals. *Langmuir, 34*(34), 10001-10011. doi:10.1021/acs.langmuir.8b01438

Table 1. Formulation and physico-chemical conditions used for the fabrication of curcumin nanoparticles by non- solvent evaporation technique.

Formulation	Native WPI (g/L)	Denatured WPI (g/L)	Curcumin (g/L)	pH	Monovalent Ionic strength (mM)
NWp	0.3	0.0	0.00	7	0.0
DWp	0.0	0.3	0.00	7	0.0
CNp-0.15	0.3	0.0	0.15	7	0.0
CNp-0.30	0.0	0.3	0.30	7	0.0
CNp-0.60	0.0	0.0	0.60	7	0.0
CDp-0.60	0.0	0.0	0.60	7	0.0
CNp-pH3.0	0.3	0.0	0.30	3	0.0
CNp-pH7.0	0.3	0.0	0.30	7	0.0
CNp-pH10.0	0.3	0.0	0.30	10	0.0
CNp-00 mM	0.3	0.0	0.30	7	0.0
CNp-40 mM	0.3	0.0	0.30	7	40
CNp- 80 mM	0.3	0.0	0.30	7	80
CNp-100 mM	0.3	0.0	0.30	7	100

Note: WPI: Whey protein isolate, NWp: Native whey protein, DWp: Denatured whey protein, CNp: Curcumin native whey protein, CDp: Curcumin denatured whey protein; Cation used is monovalent NaCl at 40, 80 and 100 mM

Figure1. Influence of processing parameter vacuum pressure (1) and solvent to non-solvent ratio (2) on the curcumin-whey protein composite nanoparticles mean size (Figure 1A) and examples of typical particle size distributions (Figure 1B). Solvent to non-solvent ratio was 1:10 (v/v), Curcumin concentration was 3 mg/L ethanol and native WPI in water (0.3 g/L) was used as stabilizer. In Fig. 1B, 35, 50, 70 and 120 represent vacuum pressure (mbar) applied during solvent evaporation. Total time taken to evaporate the solvent was 120 s at 35 mbar, 150 s at 50 mbar, 180 s at 70 mbar and 240s at 120 mbar. Error bars represent the mean ± SD of triplicate data points from three separate experiments.

Figure 2. Influence of processing parameter (solvent to non-solvent ratio) on the curcumin-whey protein composite nanoparticles mean size. Curcumin concentration was 3 mg/L ethanol and finally 0.15, 0.30 or 0.60 g/L curcumin nanoparticles were suspended in water. WPI (0.3 g/L; pH 7 and NaCl 0mM) was used as stabilizer. Solvent was evaporated at 35 mbar vacuum pressure for 120 s. Error bars represent the mean ± SD of triplicate data points from three separate experiments.

Figure 3. Influence of nucleation conditions (protein form, pH, ionic strength) on the curcumin- whey protein composite nanoparticles size (A) and surface charge (B). Solvent to non-solvent ratio was 1:10 (v/v), Curcumin concentration was 3 mg/mL ethanol and finally 0.30 g/L curcumin nanoparticles were suspended in water. Solvent was evaporated at 35 mbar vacuum pressure for 120 s; WPI either native or denatured form was used at 0.3 g/L as stabilizer. In allthe formulations, where pH was not mentioned, it was maintained at pH 7.0. Error bars represent the mean ± SD of triplicate data points from three separate experiments.

Figure 4. TEM images of negatively stained curcumin-whey protein composite nanoparticles nucleated in different physico-chemical environment. Scale bar is 0.2 µm. Solvent to non-solvent ratio was 1:10 (v/v), Curcumin concentration was 3 g/L ethanol and finally 0.30 g/L curcumin nanoparticles were suspended in water. Solvent was evaporated at 35 mbar vacuum pressure for 120 s. WPI either native or denatured form was used at 0.3g/L as stabilizer.

Figure 5. Effect of physico-chemical conditions on the intrinsic fluorescence of Trp residues of WPI (excitation wavelength = 290 nm) (5A) and interaction of WPI with curcumin (5B). In all the formulations, WPI either in native or denatured form was used at 0.3 g/L and solvent to non- solvent ratio was 1:10 (v/v). Final curcumin concentration in non-solvent was of 0.30 g/L.

Figure 6. Effect of curcumin concentration on the intrinsic fluorescence of Trp residues of WPI (excitation wavelength = 290 nm) (6A) and interaction of

curcumin with native and denatured WPI (6B). In all the formulations, WPI either in native or denatured form was used at 0.3 g/L at pH 7 and solvent to non-solvent ratio was 1:10 (v/v). Curcumin concentration was 0.15, 0.30 or 0.60 g/L which were suspended as composite particles in non-solvent. Error bars represent the mean ± SD of duplicate data points from two separate experiments.

Figure 7. Effect of formulation and emulsification conditions (native or denaturated protein, curcumin concentration, pH, ionic strength) on the mean droplet size (7A) and droplet size distribution (7B and C) of 20% oil-in-water emulsions stabilized by CWP composite nanoparticles at various physico-chemical conditions. Whey protein isolates either native ordenatured was used at 0.3 g/L as stabilizer for CWP composite nanoparticles. NWp or DWp was used as control emulsion stabilized by either native or denatured whey proteins without curcumin. Error bars represent the mean ± SD of triplicate data points from three separate experiments.

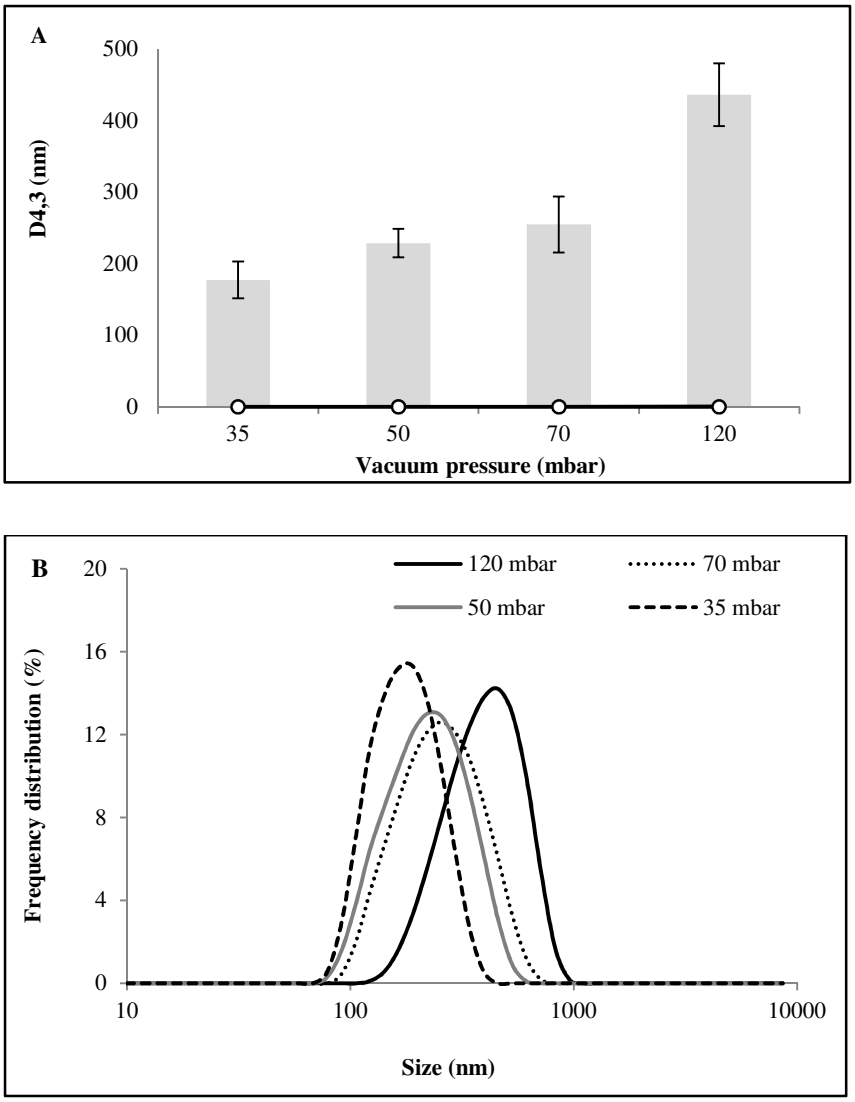
A
D4,3 (nm)
500
400
300
200
100
0
35
50
70
120
Vacuum pressure (mbar)
B
120 mbar
70 mbar
50 mbar
35 mbar
Frequency distribution (%)
20
16
12
8
4
0
10
100
1000
10000
Size (nm)

Figure 1.

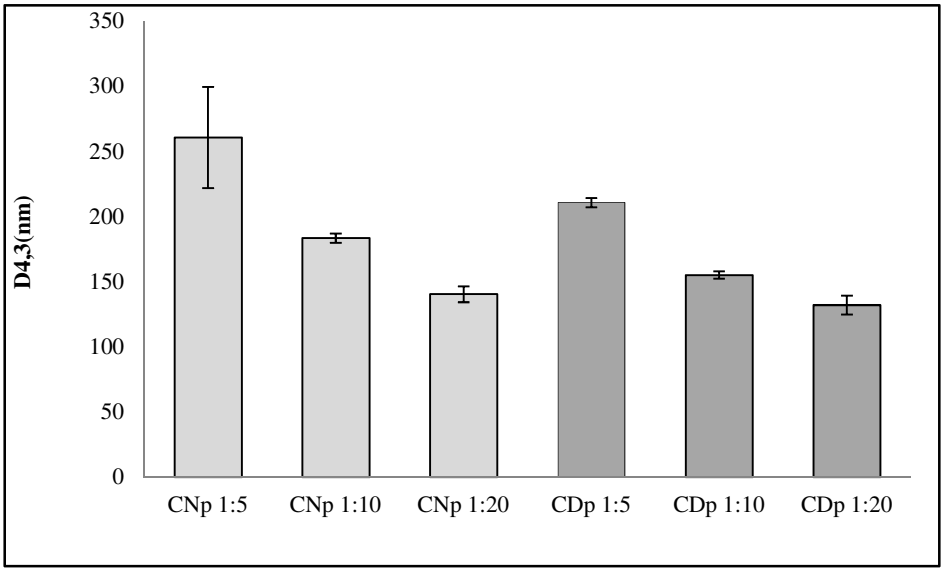
350
300
250
200
150
100
50
0
D4,3(nm)
CNp 1:5
CNp 1:10
CNp 1:20
CDp 1:5
CDp 1:10
CDp 1:20

Figure 2.

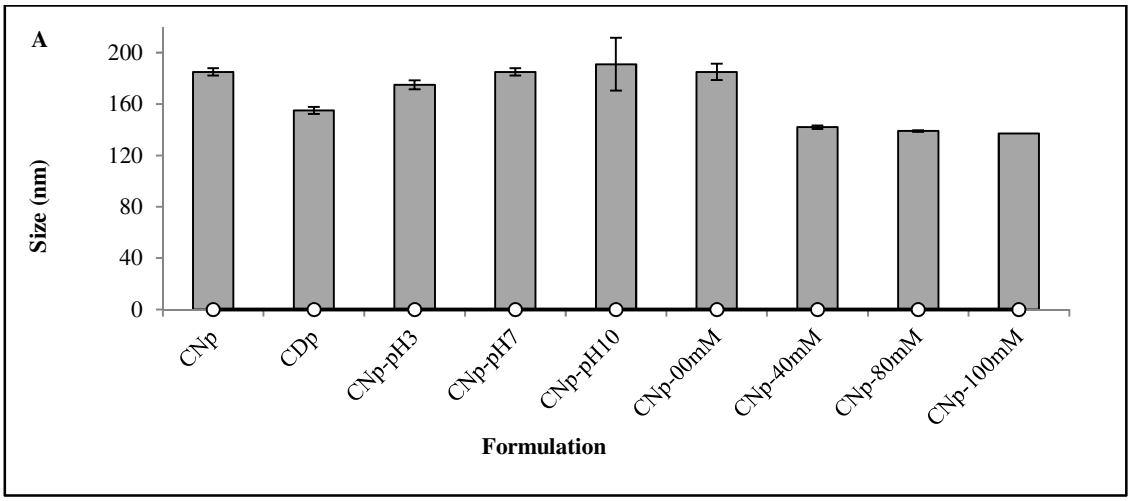
A
Size (nm)
200
160
120
80
40
0
CNp
CDp
CNp-pH3
CNp-pH7
CNp-pH10
CNp-00mM
CNp-40mM
CNp-80mM
CNp-100mM
Formulation

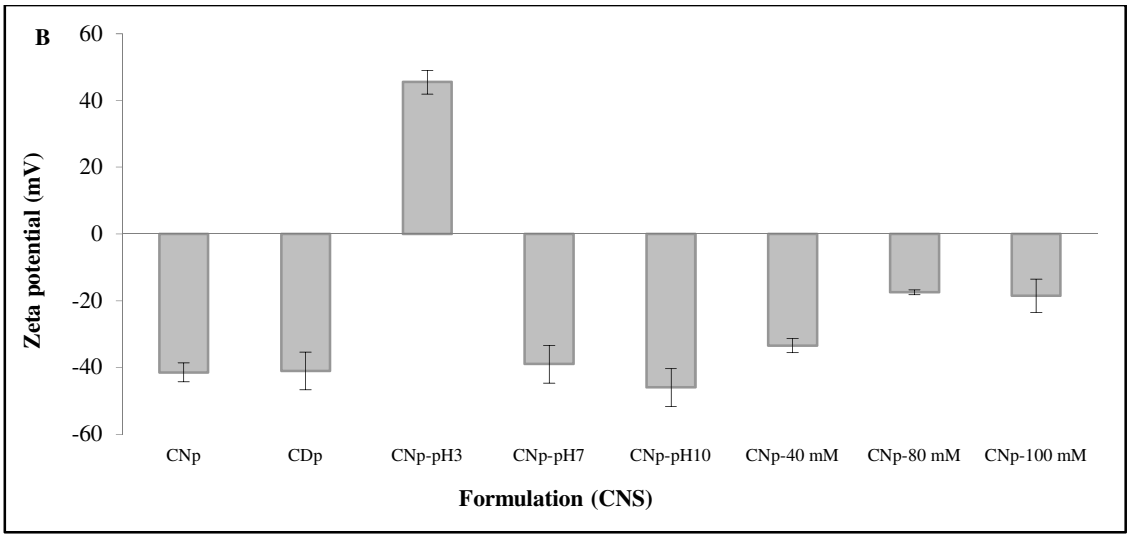
B
Zeta potential (mV)
60
40
20
0
-20
-40
-60
CNp
CDp
CNp-pH3
CNp-pH7
CNp-pH10
CNp-40 mM
CNp-80 mM
CNp-100 mM
Formulation (CNS)

Figure 3.

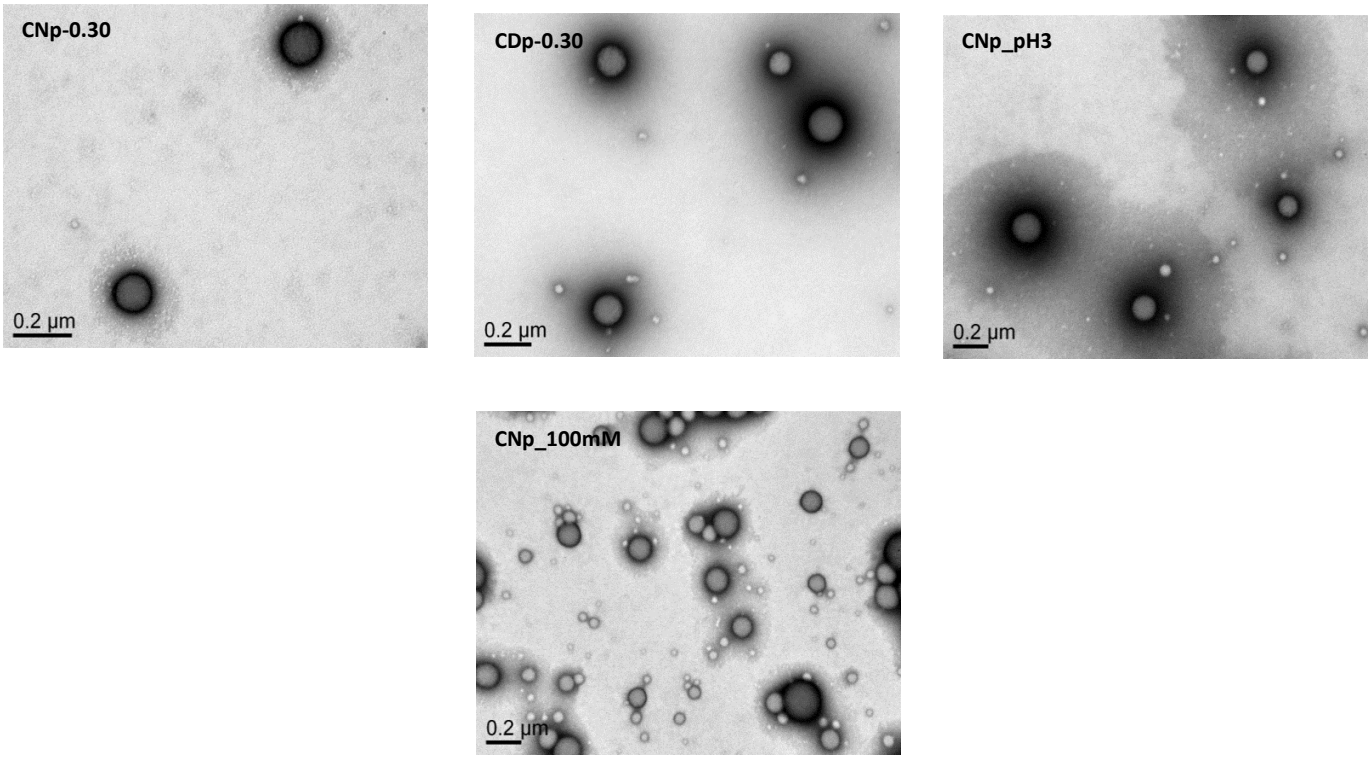

Figure 4.

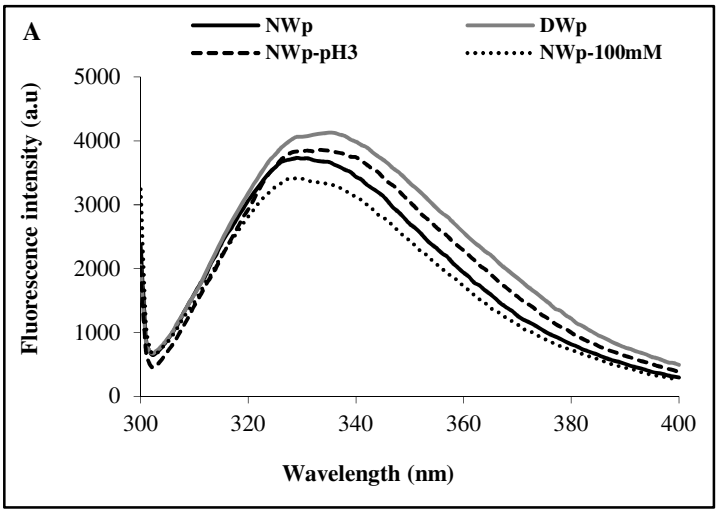
A
NWp
DWp
NWp-pH3
NWp-100mM
Fluorescence intensity (a.u)
5000
4000
3000
2000
1000
0
300
320
340
360
380
400
Wavelength (nm)

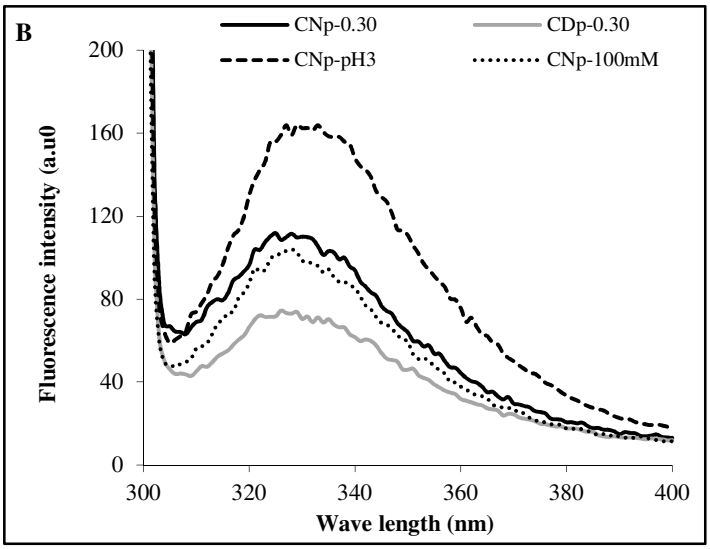
B
CNp-0.30
CDp-0.30
CNp-pH3
CNp-100mM
Fluorescence intensity (a.u0
200
160
120
80
40
0
300
320
340
360
380
400
Wave length (nm)

Figure 5.

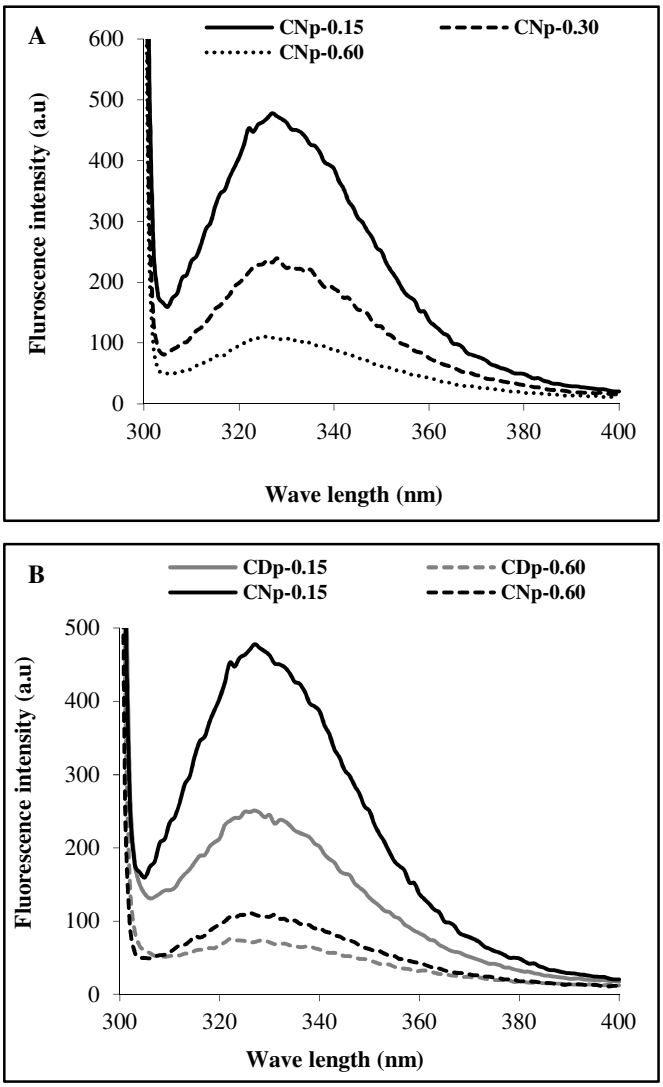
A
CNp-0.15
CNp-0.30
CNp-0.60
Fluroscence intensity (a.u)
600
500
400
300
200
100
0
300
320
340
360
380
400
Wave length (nm)
B
CDp-0.15
CDp-0.60
CNp-0.15
CNp-0.60
Fluorescence intensity (a.u)
500
400
300
200
100
0
300
320
340
360
380
400
Wave length (nm)

Figure 6.

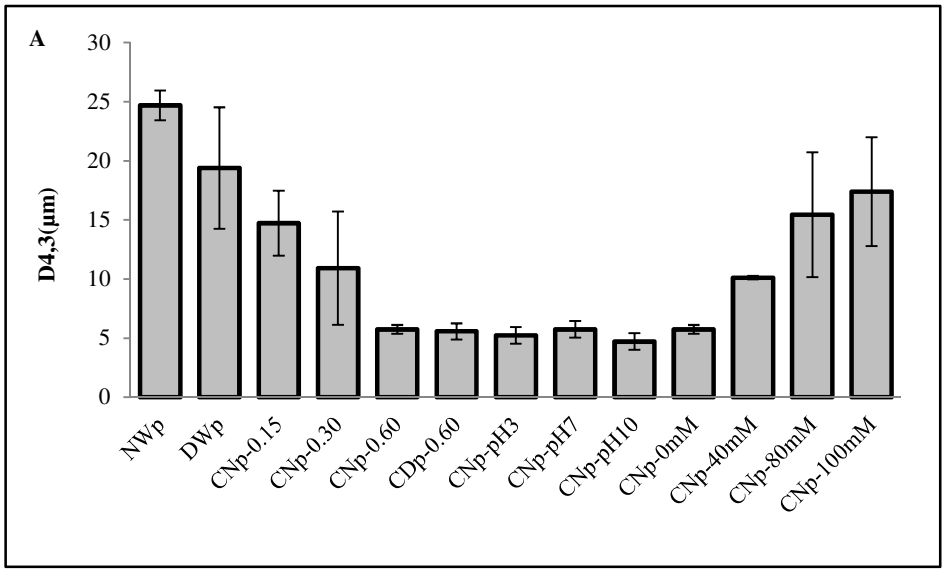
A
D4,3(µm)
30
25
20
15
10
5
0
NWp
DWp
CNp-0.15
CNp-0.30
CNp-0.60
CDp-0.60
CNp-pH3
CNp-pH7
CNp-pH10
CNp-0mM
CNp-40mM
CNp-80mM
CNp-100mM

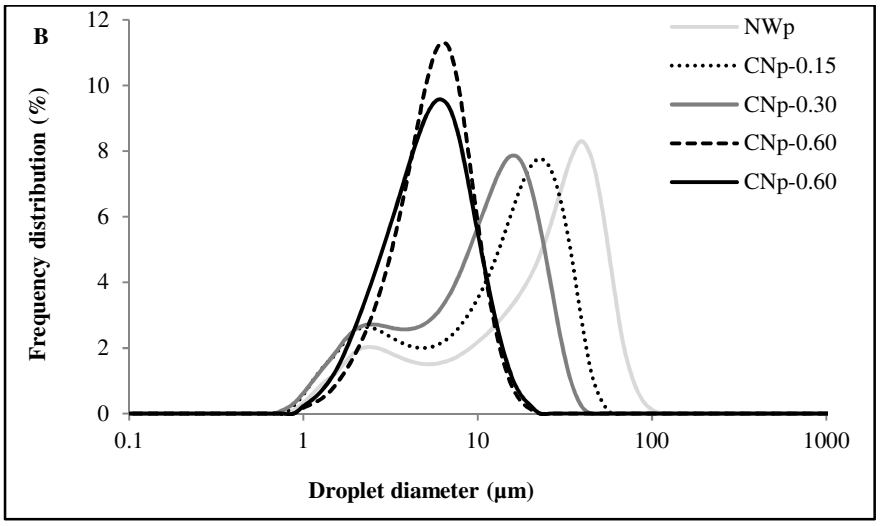
B
Frequency distribution (%)
Droplet diameter (µm)
NWp
CNp-0.15
CNp-0.30
CNp-0.60
CNp-0.60
0
2
4
6
8
10
12
0.1
1
10
100
1000

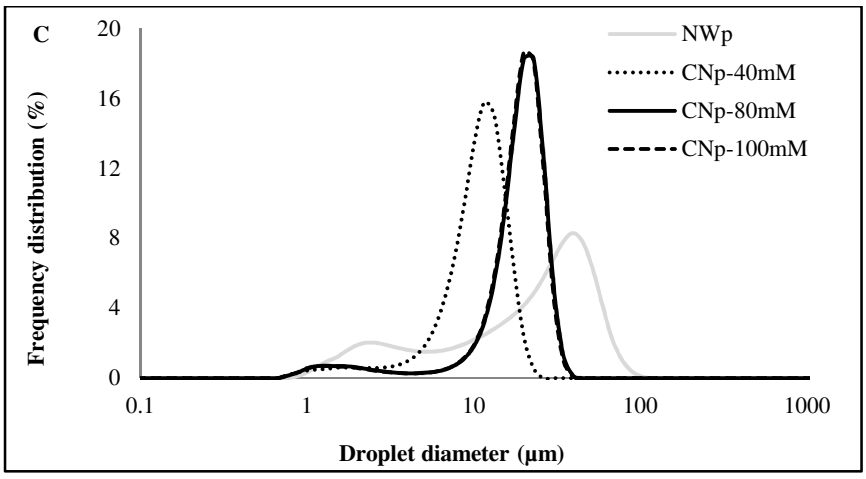
C
Frequency distribution (%)
Droplet diameter (µm)
NWp
CNp-40mM
CNp-80mM
CNp-100mM
0
4
8
12
16
20
0.1
1
10
100
1000

Figure 7.